A Visco-Elastic Model for Groundwater Level Changes in Cho-Shui River Alluvial Fan after the Chi-Chi Earthquake in Taiwan

Yun-Bin Lin [a], Yih-Chi Tan [b*], Tian-Chyi Jim Yeh [c], Chen-Wuing Liu [b], Chu-Hui Chen [d]

[a] *Council of Agriculture, Executive Yuan, Taipei 100, and Department of Bioenvironmental Systems Engineering, National Taiwan University, Taipei 10617, Taiwan, R.O.C.*

[b] *Department of Bioenvironmental Systems Engineering, and Hydrotech Research Institute, National Taiwan University, Taipei 10617, Taiwan, R.O.C.*

[c] *Department of Hydrology and Water Resources, University of Arizona, Tucson, AZ 85721, USA*

[d] *Department of Civil Engineering, ChungKuo Institute of Technology, Taipei 106, Taiwan, R.O.C.*

*Corresponding Author
Tel: +886-2-2369-0342
Fax: +886-2-2369-8630
E-mail address: yctan@ccms.ntu.edu.tw

Abstract

A visco-elastic model is developed to simulate the ground water level changes in the Cho-Shui River alluvial fan in Taiwan after the Chi-Chi earthquake. An analytical solution is derived with the assumption that no leakage occurred in confined aquifers during the co-seismic period. The solution is used to analyze the data collected from a high-density network of hydrologic monitoring wells in the Cho-Shui River alluvial fan. The simulated ground water level changes agree with the observations. The viscosity coefficient of the model was found to correlate with the hydraulic conductivity of the aquifer. The field observations and the simulations reveal the influence of geological structures and heterogeneity on the ground water changes and locations of sediment liquefactions in the alluvial fan during the Chi-chi earthquake. Possible applications to imaging subsurface hydraulic heterogeneity are discussed using information about ground water level changes induced by earthquakes.

Keywords Chi-Chi earthquake, Groundwater level changes in wells, Visco-elastic model, Delineation, Sand/gravel formation.

1. Introduction

At 01:47'12.6" on September 21, 1999, an earthquake of magnitude 7.3 on the Richter scale (M_L) occurred in the middle of Taiwan, caused by the motion of the Chelungpu thrust fault. The epicenter was located at 23.87°N and 120.75°E, near the town of Chi-Chi, which is about 10 km away from the Cho-Shui River alluvial fan [Ma et al., 1999; Yu et al., 2001]. A second earthquake of a magnitude of 6.9 took place at 19:52'50.0" on September 26, 1999 with the epicenter at 23.86°N and 121.00°E. The Cho-Shui River alluvial fan is located in the mid-western plan of Taiwan and has an area about 1700 km^2. A series of west-vergent thrust faults and anticlines have been mapped near the eastern side of the fan (Figure 1). The Cho-Shui River flows from east to west through two anticlines, the Dulliu and Baqua hills [Lin et al., 2000, 2001], and is the main recharge area of the fan. A Groundwater Monitoring Network System (GMNS), has been established at the fan since 1992. The network consists of 70 evenly distributed hydrological stations, where a total of 188 monitoring wells are installed at various depths from 24 to 306 m. Each well is screened at only one depth, and the water levels at all of the wells have been recorded automatically at every hour [Hsu, 1998]. The records of the GMNS showed the ground water level rises ranged from 1 m to 7 m and falls from -2 m to –11 m before and after these two earthquakes [Water Conservancy Agency, 1999a].

During the past few decades, efforts have been made to identify the relation

between field strain and ground water level changes caused by earthquakes. Numerous studies [Roeloffs, 1996] have suggested that the poro-elastic theorem by Biot [1956a, 1956b] can be used to describe the local pore pressure change induced by earthquakes. Many attempts also have been made to use the ground water level change as a pre-cursor of the earthquake [Ohno, 1997]. However, because of insufficient monitoring wells [Roeloffs, 1998] and the scale-disparity between models and the aquifer [Grecksch et al., 1999], the relation between earthquakes and changes in groundwater levels remains uncertain.

The well-instrumented well fields in the fan and the vast amount of data recorded by the GMNS during the Chi-Chi earthquakes provide a unique opportunity to study the relation between earthquakes and ground water level changes. The objective of this study is to construct a mathematical model to describe and understand the ground water level changes after the Chi-Chi earthquakes in the Cho-Shui River alluvial fan. Specifically, we developed a visco-elastic model based on the local hydrogeological condition of the alluvial fan, derived an analytical solution of the model, and used it with field data to simulate the evolution of the ground water level changes after the earthquakes. Finally, we discussed the importance of geological structures, and heterogeneity on the observed ground water level changes and sediment liquefaction during the earthquakes. Possible applications of the model to identification of aquifer heterogeneity are also explored.

2. Theory of Propagation of Elastic Waves in Aquifers

Hassanizadeh and Gray [1979a, 1979b, 1980] adopted the method proposed by Coleman and Noll [1963] to linearize the momentum equations of the two-phase flow by employing the entropy inequality of thermodynamics. Linearized momentum equations of the liquid phase and the solid phase can be expressed as

$$\left(1-\varepsilon_f\right)\rho^s\frac{\partial^2 u_k^s}{\partial t^2}-\left(1-\varepsilon_f\right)\rho^s g_k^s+\left(1-\varepsilon_f\right)\nabla_k p^f-\sigma_{kl,l}^s+R^f\upsilon_k^d=0\,, \tag{1a}$$

and

$$\varepsilon_f\rho^f\frac{\partial^2 u_k^f}{\partial t^2}-\varepsilon_f\rho^f g_k^f+\varepsilon_f\nabla_k p^f-R^f\upsilon_k^d=0 \tag{1b}$$

respectively, with the assumptions that: 1) there is no phase change; 2) the fluid phase is macroscopically non-viscid; 3) the temperature gradient is considered only as heat conduction; 4) the acceleration of the convection term is neglected; and 5) the capillary effect is negligible. In equations (1a) and (1b), ε_α is the void fraction with respect to the α phase, (f denotes the liquid phase, and s the solid phase; ρ^α represents intrinsic mass density of the α phase [M/L^3]; u_k^α is the displacement vector of the α phase in the k direction [L]; g is the gravity [L/T^2]; $\nabla_k p^f$ denotes pressure gradient of the liquid phase in the k direction [M/(L^{3}T^2)]; $\sigma_{kl,l}^s$ denotes the stress tensor gradient with respect to the solid phase in l direction [$\mathrm{M}/\left(\mathrm{L}^3\mathrm{T}^2\right)$]; R^f is a linear coefficient tensor describing the momentum exchange due to the relative velocity of the liquid phase and the solid phase [M/(L^{3}T)]. The coefficient tensor becomes a scalar whenever the reference coordinates are parallel to the principle axes of the equations. The term υ_k^d is the relative velocity vector of the liquid and solid phases in the m direction

[L/T].

When equations (1a) and (1b) are used to describe the propagation of elastic waves in fluid-saturated porous media, Biot [1956a, 1956b], Berryman et al. [1988], and Jeng and Lee [2001] showed that an extra term is needed to fully represent the dynamic behavior of the media. The term is related to the relative acceleration of the liquid and solid phases. After adding this term, the momentum equations become

$$\left(1-\varepsilon_f\right)\rho^s \frac{\partial^2 u_k^s}{\partial t^2} - \left(1-\varepsilon_f\right)\rho^s g_k^s + \left(1-\varepsilon_f\right)\nabla_k p^f - \sigma_{kl,l}^s + R^f \upsilon_k^d + A^s a_k^d = 0\,, \quad \text{(2a)}$$

and

$$\varepsilon_f \rho^f \frac{\partial^2 u_k^f}{\partial t^2} - \varepsilon_f \rho^f g_k^f + \varepsilon_f \nabla_k p^f - R^f \upsilon_k^d - A^s a_k^d = 0\,. \quad \text{(2b)}$$

In which A^s is an additional apparent mass density of the solid phase [M/L^3]; and a_k^d represents the relative acceleration of the liquid phase to the solid phase in the m direction [L/T^2]. Equations (2a) and (2b) can be compared with the coupled momentum equations for solids and fluids of Biot's theory of propagation of elastic waves in a fluid-saturated porous medium:

$$\frac{\partial^2}{\partial t^2}\left(\rho_{11} u_k^s + \rho_{12} u_k^f\right) + \left(1-\varepsilon_f\right)\nabla_k p^f - \sigma_{kl,l}^s - b\upsilon_k^d = 0 \quad , \quad \text{(3a)}$$

and

$$\frac{\partial^2}{\partial t^2}\left(\rho_{12} u_k^s + \rho_{22} u_k^f\right) + \varepsilon_f \nabla_k p^f + b\upsilon_k^d = 0 \quad \text{(3b)}$$

where the coefficient b is related to the intrinsic permeability, κ [L^2], the fluid viscosity, μ [M/(LT)], and the porosity as $b = \mu {\varepsilon_f}^2 / \kappa$. Here the gravity term is also omitted if a horizontal plane model is considered. The comparison yields that 1) $\rho_{12} = A^s$, $\rho_{11} = \rho^s \varepsilon_s - A^s$ and $\rho_{22} = \rho^f \varepsilon_f - A^s$; 2) $b = R^f$; 3) $\rho_{11} + \rho_{12}$ is thus equal to the bulk

density of the solid phase pr unit volume of the porous media, $\varepsilon_s \rho^s$; 4) $\rho_{12} + \rho_{22}$, is equivalent to the bulk density of the liquid phase per unit volume of the porous media, $\varepsilon_f \rho^f$; and 5) the term, a_k^d, is equal to $\frac{\partial^2}{\partial t^2}(u_k^f - u_k^f)$.

If equations (3a) and (3b) are isotropic functions, the representation theorem [Wang, 1970a, 1970b; Drew and Passman, 1999] explains the necessity of the term, A^s. Based on the representation theorem, an isotropic function should include all the objective variables (variables that can be regarded as objective variables only when their values are frame-indifferent). Because of a_k^d is an objective variable, $A^s a_k^d$ should be included in (2a) and (2b) such that the isotropic property of the equations can be fully specified. Physically, the term, ρ_{12}, can be regarded as an additional mass, induced by the oscillation of solid particles in the liquid phase. A similar theorem explaining an apparent mass induced by a rigid body oscillating in the fluid can also be found in the potential flow theorem of the fluid mechanics [Lamb, 1945].

Using the Lagrangian formulation, Berryman et al. [1988] developed a complete theory of elastic wave propagation in partially saturated porous media. Equations of motion were derived for solid, liquid, and gaseous constituents, including the effects of their interactions. Assuming the effects of capillary pressure changes are negligible, Berryman et al. [1988] showed that the equations can be simplified to a form similar to Biot's equations. Using the Helmholtz transformation, they decoupled the equations into

$$\nabla^2 \chi = \frac{k_s^2}{w^2} \frac{\partial^2 \chi}{\partial t^2} \tag{4a}$$

for one distortional wave and

$$\nabla^2 A_{\pm} = \frac{k_{\pm}^2}{w^2} \frac{\partial^2 A_{\pm}}{\partial t^2} \tag{4b}$$

for two dilatational waves. In equations (4a) and (4b), A_+ is a scalar potential for the solid phase with the faster wave speed, and A_- is a scalar potential for the liquid phase with the slower wave speed; k_s, *and* $k_{\pm}$ are wave vectors [1/L]; χ is a vector potential for the solid phase; and w is the vibration frequency [1/T].

If we assume equation (3a) and (3b) are isotropic and take the divergence of the equations, we have

$$\nabla^2 \sigma^s - (1-\varepsilon_f)\nabla^2 p^f + \nabla p^f \cdot \nabla \varepsilon_f = \frac{\partial^2}{\partial t^2}(\rho_{11} e + \rho_{12} \varsigma) - b \frac{\partial}{\partial t}(\varsigma - e) - \upsilon^d \nabla \cdot b \text{ , and} \tag{5a}$$

$$-\varepsilon_f \nabla^2 p^f - \nabla p^f \cdot \nabla \varepsilon_f = \frac{\partial^2}{\partial t^2}(\rho_{12} e + \rho_{22} \varsigma) + b \frac{\partial}{\partial t}(\varsigma - e) + \upsilon^d \nabla \cdot b \text{ ,} \tag{5b}$$

where $e = \nabla \cdot u_k^s$ and $\varsigma = \nabla \cdot u_k^f$. According to the Biot theorem, the pore pressure obeys the diffusion equation in the poro-elastic model. The summation of equation (5a) and (5b) leads to

$$\nabla^2 \left[\left(\sigma^s - \varepsilon_s p^f \right) - \varepsilon_f p^f \right] = \frac{\partial^2}{\partial t^2} \left[(\rho_{11} + \rho_{12}) e + (\rho_{22} + \rho_{12}) \varsigma \right]. \tag{6}$$

Using the mixture theorem [Green and Naghdi, 1965], we can express equation (6) as two wave equations:

$$\nabla^2 \left(\sigma^s - \varepsilon_s p^f \right) = \frac{\partial^2}{\partial t^2} \left[(\rho_{11} + \rho_{12}) e \right] = \rho^s \frac{\partial^2}{\partial t^2} (\varepsilon_s e) \cong \rho^s \frac{\partial^2}{\partial t^2} \left[\nabla \cdot \left(\varepsilon_s u^s \right) \right] \tag{7a}$$

$$\nabla^2 \left(-\varepsilon_f p^f \right) = \frac{\partial^2}{\partial t^2} \left[(\rho_{22} + \rho_{12}) \varsigma \right] = \rho^f \frac{\partial^2}{\partial t^2} \left(\varepsilon_f \varsigma \right) \cong \rho^f \frac{\partial^2}{\partial t^2} \left[\nabla \cdot \left(\varepsilon_f u^f \right) \right]. \tag{7b}$$

This theorem implicitly assumes that terms such as $\nabla p^f \cdot \nabla \varepsilon_f$, $\frac{\partial^2}{\partial t^2}\left(-\rho_{12} e + \rho_{12} \varsigma\right)$ and $\upsilon^d \nabla \cdot b$ are small compared with the other terms in equations (5a) and (5b), and they can be neglected in equations (5a) and (5b) during the co-seismic motion period. Because of the omission of the term, $\frac{\partial^2}{\partial t^2}\left(-\rho_{12} e + \rho_{12} \varsigma\right)$, equations (7a) and (7b) are quasi-static descriptions of equations (5a) and (5b). Additionally, the $b\frac{\partial}{\partial t}\left(\varsigma - e\right)$ term is omitted in the summation but its effect can be included using a constitutive equation to be discussed later.

Prevost [1982] suggested that a single-phase description of porous media behavior is adequate when the loading rate is much higher than the diffusion rate. This implies that if no efflux of the pore fluid from porous media takes place during the co-seismic motion period and the fluid is compressible, then only equation (7b) is needed for describing the dynamics of wave propagation in the porous media. As a result, we assume that no leakage occurs from one confined aquifer to another in the fan during the co-seismic compression (this is supported by hydrogeological data supplied by The Central Geological Survey [1994, 1999], shown in Figure 2), and we can use only equation (7b) in our following analysis.

Suppose that the liquid phase in our study area obeys the Maxwell-Fluid model (see Figure 2) [Flħgge, 1975], a constitutive relationship between the stress and the strain can be used for describing the pore pressure dissipation caused by the relative velocity of the liquid phase and the solid phase:

$$\left(-\varepsilon_f p^f\right) + \frac{\eta}{C}\frac{\partial}{\partial t}\left(-\varepsilon_f p^f\right) = \eta \frac{\partial}{\partial t}\left[\nabla \cdot \left(\varepsilon_f u^f\right)\right]. \tag{8}$$

In equation (8), the viscosity coefficient, η [M/(LT)], is defined as the ratio of the pressure to the strain rate and C is the bulk modulus of the liquid phase [M/(LT^2)]. The advantage of using equation (8) is that knowledge of the exact motion of the solid phase is not necessary, which is implicitly included in the viscosity coefficient in equation (8). The coefficient can be related to well-defined parameters, such as hydraulic conductivity.

For one-dimensional model, the horizontal displacement of the liquid phase per unit volume of the porous medium can be expressed as

$$\varepsilon_f u^f = \xi e^{-\gamma x} e^{i(lx-wt)}, \tag{9}$$

where ξ is a constant [L]; γ is an attenuation coefficient [1/L]; x is the distance [L]; l is the wave vector, [1/L], and w is the vibration frequency [1/T]. The strain of the liquid phase per unit volume of the porous media then is

$$\nabla \cdot \left(\varepsilon_f u^f\right) = \left(-\gamma + li\right)\left(\varepsilon_f u^f\right). \tag{10}$$

The strain rate of the liquid phase per unit volume of the porous media therefore becomes

$$\frac{\partial \nabla \cdot \left(\varepsilon_f u^f\right)}{\partial t} = -iw\left(\varepsilon_f u^f\right)\left(-\gamma + li\right). \tag{11}$$

In addition, we express the relationship between the strain rate of the liquid phase per unit porous media and the stress of the liquid phase per unit porous media as

$$\Lambda \frac{\partial \nabla \bullet \left(\varepsilon_f u^f\right)}{\partial t} = -\varepsilon_f p^f. \tag{12}$$

Substituting this relation into equation (8), we obtain

$$\Lambda = \frac{\eta}{\left(1 - \frac{w\eta i}{C}\right)} \ . \tag{13}$$

According to equation (12) and (13), the phase of the pore pressure per unit volume of the porous media has a lag of $\theta = \tan^{-1}\left(\frac{w\eta}{C}\right)$ behind the phase of the strain rate of the liquid phase per unit volume of the porous media. Upon substituting equations (10), (11), (12) and (13) into (7b), equation (7b) becomes

$$\frac{-w\eta i}{\left(1 - \frac{w\eta i}{C}\right)} \nabla^2 \left(\varepsilon_f u^f\right) = \rho^f \frac{\partial^2}{\partial t^2}\left(\varepsilon_f u^f\right). \tag{14}$$

Comparing (14) with (4b), we can set $A_{\_} = \varepsilon_f u^f$ to get $k_{\_}^2 = \frac{w^2}{v_f^{\ 2}}\left(1 + Qi\right)$ where $Q = \frac{C}{w\eta}$.

From equation (9), we can show that

$$\frac{\partial^2}{\partial t^2}\left[\left(\varepsilon_f u^f\right)\right] = -i\omega \frac{\partial}{\partial t}\left[\left(\varepsilon_f u^f\right)\right]. \tag{15}$$

Using equation (15) in equation (14), equation (14) can be expressed as

$$\frac{\partial^2 A_{\_}}{\partial x^2} - \frac{\rho^f}{\eta}\frac{\partial A_{\_}}{\partial t} - \frac{1}{v_f^{\ 2}}\frac{\partial^2 A_{\_}}{\partial t^2} = 0\,, \tag{16}$$

where $v_f = \sqrt{C/\rho^f}$ is the velocity of the wave propagation in the liquid phase. Depending on the equation (11), (12), and (13), the pressure per unit volume of the fluid can be expressed in the similar form as equation (16). This is our visco-elastic model to be used in the following analysis. The visco-elastic model considers the inertial effect that is neglected in the pore-elastic model. Eringen [1980] and Bardet [1992] showed that a visco-elastic model, instead of the poro-elastic model, can describe the dynamic response of the saturated porous

media.

3. Hydrogeology of the Study Area

The Cho-Shui River's alluvial fan consists of several layers of Holocene to Pleistocene sands and gravels that formed the three aquifers separated by marine mud [Central Geological Survey, 1994, 1999]. The rising and falling mean sea levels caused by global climate change late in the Quaternary Period formed the layered structure of the alluvial fan. Massive gravels are laid at the upper fan and thinning out towards the west of the fan, while the mud layers thicken.

The Central Geological Survey [1994, 1999] constructed 12 hydrogeological profiles for the alluvial fan; three aquifers (Aquifer 1, Aquifer 2, and Aquifer 3) were identified in the analysis of the profiles (Figure 2(a)). Aquifer 2 can be divided horizontally into a confined part on the tail fan, a partially confined part on the mid fan and an unconfined part on the upper fan. Gravelly sediments were found on the mid-upper fan and in the partially confined and unconfined part of the aquifers, while arenaceous sediments were found only in the confined parts of the aquifer. Furthermore, an interface between the gravels and the arenaceous sediments was identified to separate the partially confined part from the confined part of the aquifers. The confined portion pinches out below the shoreline (Figure 2(b)).

Rupturing of the Chelungpu fault in the Chi-Chi earthquake led to several meters of oblique thrust of the hanging wall relative to the footwall. According to GPS measurements, only minor subsidence (< 0.5 m) was observed in the Cho-Shui River alluvial fan after the Chi-Chi earthquake [Department of Land Administration, 2000]. The ground water level in the Cho-Shui river alluvial fan, however, changed as much as ±10 m right after the Chi-Chi earthquake [Chia et al., 2000; Water Conservancy Agency, 2000]. The spatial distribution of general ground water level changes (i.e. rises and declines) between 01:00 and 02:00 on Sep. 21 are shown in Figure 3. Based on this figure, negative water level changes were recorded in wells located in a narrow, belted area between the Chelungpu and Changhwa thrust faults. This volumetric expansion zone in the footwall perhaps is caused by the dragging effect of thrusting. Wells that recorded positive water level changes are generally located further away from the ruptured fault. The magnitude of the rise of the water level tends to increase from the upper fan toward the mid fan, and then decrease toward the tail fan [Chia, 2001; Wang, 2001; Lee, 2002]. The ground water levels in wells adjacent to the western side of the Changwha thrust fault declined in one aquifer and rose in all the other aquifers. Such a distribution of ground water level changes was found inconsistent with the calculated strain fields reported by Ma [2001] and Huang [2000]. The inconsistency appears to suggest that ground water levels may also be affected by the hydrological heterogeneity in the aquifers in the fan in addition to the forces of the earthquake.

4. Conceptual Model for the Study Area

The Chelungpu fault ruptured from the south to the north during the Chi-Chi earthquakes and induced pressure waves, propagating from east to the west and almost parallel to the contour lines of the groundwater levels recorded before the earthquakes. Therefore, the 85 km long rupture zone that formed during the Chi-Chi earthquakes was considered supplying a western-eastern direction pressure pulse simultaneously to the fan (Figure 3). In view of the time scale of the model (daily average) and the dozens of second co-seismic periods, the pressure induced by the earthquake is treated as an impulse pressure. Suppose that no leakage took place from the confined part to other aquifers during the co-seismic compression. Since the thickness of the aquifer decreases from east to west, conservation of momentum suggests that when the wave propagates from east to west, the change of the velocity will be significant towards the pinch-out of the aquifer. Thus, the inertial influence on the ground water level fluctuations increases. The inertial term must be considered at the western side of the interface; our visco-elastic model, equation (16), thus will apply. Conversely, based on the physical properties of gravelly aquifers and the hydro-geological structure of the aquifers, the fluid behavior after the earthquake at the eastern side of the interface is assumed to obey the diffusion equation.

To use equation (16) to describe the motion of the fluid phase within the arenaceous

confined aquifer, the boundary conditions of equation (16) are set to be a zero strain rate at the pinch-out ($x=L$, the distance between the interface and the pinch-out) and an impulse pressure at the interface ($x=0$) (see Figure 2(c)). The initial conditions for equation (16) are

$$A_{-}(x,0)=\frac{\partial}{\partial t}A_{-}(x,0)=0\,. \tag{17}$$

Equation (17) implies that the velocity and displacement of the liquid phase are zero before the earthquake.

Taking the Laplace transformation of equation (16) to project t into s and $A_{-}(x,t)$ into $\overline{A_{-}}(x,s)$, and then employing the initial conditions, equation (17) becomes

$$\overline{A_{-}}''(x,s)-\frac{\rho^{f}}{\eta}s\overline{A_{-}}(x,s)-\frac{1}{v_{f}^{\,2}}s^{2}\overline{A_{-}}(x,s)=0\,. \tag{18}$$

We assume the solution take the form

$$\overline{A_{-}}=M(s)e^{\lambda x}\,. \tag{19}$$

After substituting equation (19) into equation (18), we have

$$\lambda=\pm\sqrt{\frac{\rho^{f}}{\eta}s\left(1+\frac{\eta}{C}s\right)}=\pm\frac{1}{v_{f}}\sqrt{s\left(\frac{C}{\eta}+s\right)}\,. \tag{20}$$

Because when $x\to\infty$, $\overline{A_{-}}\to 0$, the negative λ value is the correct solution.

When the impulse pressure $P\delta(t)$ is applied at $x=0$ and $t=0$, the strain at $x=0$ is

$$A_{-}'(0,t)=P\delta(t)\frac{\frac{\eta}{C}+t}{\eta}\,. \tag{21}$$

The Laplace transform of equation (21) yields

$$\overline{A_-}'(0,s) = P\frac{1}{C} = \lambda M(s). \tag{22}$$

After M(s) is determined using the boundary condition, it is substituted into equation (19). We then have

$$\overline{A_-}(x,s) = -\frac{Pv_f}{C\sqrt{s\left(\frac{C}{\eta}+s\right)}} e^{-\frac{x}{v_f}\sqrt{s\left(\frac{C}{\eta}+s\right)}}. \tag{23}$$

The Laplace transformation of $f(t) = I_0\left(\varpi\sqrt{t^2-\xi^2}\right)H(t-\xi)$ is $\overline{f}(s) = \frac{1}{\sqrt{(s-\varpi)(s+\varpi)}} e^{-\xi\sqrt{(s-\varpi)(s+\varpi)}}$ [Farrell and Ross, 1971]. Meanwhile, the translation property projects $f(t) = I_0\left(\varpi\sqrt{t^2-\xi^2}\right)e^{-\varpi t}H(t-\xi)$ into $\overline{f}(s) = \frac{1}{\sqrt{s(s+2\varpi)}} e^{-\xi\sqrt{s(s+2\varpi)}}$. Using $\varpi = \frac{C}{2\eta}$ and $\xi = \frac{x}{v_f}$ in equation (18), the transverse Laplace transformation of equation (23) can be expressed as

$$A_-(x,t) = -\frac{Pv_f}{C} I_0\left(\frac{C}{2\eta}\sqrt{t^2-\left(\frac{x}{v_f}\right)^2}\right) e^{-\frac{C}{2\eta}t} H\left(t-\frac{x}{v_f}\right). \tag{24}$$

The pore pressure per unit volume of the porous media can be obtained by applying equation (24) to equation (11) and expressed as

$$\varepsilon_f p^f = \frac{Pe^{-\beta t}}{\left(1+\left(\frac{1}{Q}\right)^2\right)} \frac{x}{v_f}\left\{\frac{tI_1(\Theta)}{2\Delta^{3/2}} - \frac{CI_1(\Theta)}{4\eta\Delta^{1/2}} - \frac{C}{8\eta}\frac{t\left[I_0(\Theta)+I_2(\Theta)\right]}{\Delta}\right\} H\left(t-\frac{x}{v_f}\right) + Z, \tag{25}$$

where $\Delta = t^2 - \left(x/v_f\right)^2$; $H(\ )$ is the Heaviside function; $\Theta = \beta\sqrt{\Delta}$; $\beta = C/(2\eta)$; $I_n(\ )$ is the nth order Bessel function.

The constant Z introduced by the phase lag in equation (25) can be obtained by

applying the boundary condition of zero strain rate, that is, $\frac{\partial}{\partial t}\left(\nabla \cdot A\_\left(L,t\right)\right) = -\frac{\varepsilon_f p^f}{\Lambda} = 0$. Therefore, the pore pressure per unit volume of the porous media induced by unit pressure, $Unit^f\left(x,t\right)$ when $t > (x/v_f)$, is given as

$$Unit^f\left(x,t\right) = \frac{e^{-\beta t}}{\left(1+\left(\frac{1}{Q}\right)^2\right)}\left\{\begin{array}{l}\left\{\frac{tI_1(\Theta)}{2\Delta^{3/2}} - \frac{CI_1(\Theta)}{4\eta\Delta^{1/2}} - \frac{C}{8\eta}\frac{t\left[I_0(\Theta)+I_2(\Theta)\right]}{\Delta}\right\}\left(\frac{x}{v_f}\right) \\ -\left\{\frac{tI_1(\Theta_L)}{2\Delta_L^{3/2}} - \frac{CI_1(\Theta_L)}{4\eta\Delta_L^{1/2}} - \frac{C}{8\eta}\frac{t\left[I_0(\Theta_L)+I_2(\Theta_L)\right]}{\Delta_L}\right\}\left(\frac{L}{v_f}\right)\end{array}\right\} H\left(t-\frac{x}{v_f}\right) \quad (26)$$

where $\Delta_L = t^2 - \left(L/v_f\right)^2$; $\Theta_L = \beta\sqrt{\Delta_L}$. From equation (26), when η is smaller, the pore pressure dissipates faster.

In order to apply the solution, equation (26), to the study area, the pressure impulse at the interface between the gravels and sands must be specified. To resolve this issue, we use the following approach. The force F of the earthquake leads to a sudden lifts in pore pressure at the interface. Based on Biot's derivation [Biot, 1941; Ge and Stover, 2000] and our knowledge of the geohydrology of the fan, whenever the force F is removed, the dissipation of the pore pressure, $\varepsilon_f p_{bc}^f$, on the eastern side of the interface will obey the diffusion equation,

$$\frac{\partial\left(-\varepsilon_f p_{bc}^f\right)}{\partial t} = \frac{K}{S_s}\frac{\partial^2\left(-\varepsilon_f p_{bc}^f\right)}{\partial x^2} + \frac{F}{B}\delta(x)\delta\left(t-t'\right), \quad (27)$$

where S_s is the specific storage [1/L]; K is the hydraulic conductivity of the aquifer [L/T]; and B is the thickness of the aquifer. If the initial condition is give as $p_{bc}^f(x,0) = 0$. The corresponding solution for an unbounded medium is

$$p_{bc}^{f}\left(x,t\right)=-\frac{\frac{F}{B}\exp\left[-\left(\frac{x^{2}S_{s}}{4Kt}\right)\right]}{2\varepsilon_{f}\sqrt{\pi t\left(K/S_{s}\right)}}. \tag{28}$$

When the impulse pressure is applied on the liquid phase, the displacement takes place simultaneously along the direction of the force and the energy associated with the impulse is transmitted via the wave propagation from the upper fan to the tail fan. The geological structures and heterogeneity caused the high pore pressure at the interface in the aquifer. Because of the unbalanced pressure head, the liquid phase flows from high to low pressure. After the impulse pressure was removed, ground water flowed from the interface of the sands and the gravels to both upstream and downstream of the Cho-Shui River alluvial fan after the Chi-Chi earthquake. The energy is proportional to square of the displacement, the displacement will decrease with the time and distance of the wave propagation because of the viscosity between the liquid phase and the solid grains. If the upstream flow obeys the diffusion equation, then the change in the pore pressure at the interface, *x=0*, is

$$p_{bc}^{f}\left(0,t\right)=\frac{1}{2\varepsilon_{f}\sqrt{\pi t}}\frac{F/B}{\sqrt{\left(K/S_{s}\right)}}. \tag{29}$$

The pore pressure in the arenaceous sediments, p_{res}^{f}, therefore can be expressed as the convolution form of p_{bc}^{f} and $Unit^{f}$ as

$$p_{res}^{f}\left(x,t\right)=\int_{0}^{t}p_{bc}^{f}\left(0,t\right)Unit^{f}\left(x,t-\tau\right)d\tau. \tag{30}$$

5. Results and Discussion

To apply the model to the study area, observed groundwater levels from four sets of wells are used (Figure 4). Each well set consists of one well on the east side of the interface and the other on the west side. Each well is labeled using a number followed by a letter and another number (e.g., 3W1). The first number denotes the aquifer where the well is screened (i.e. 3 for Aquifer 3); the second letter indicates the location of the well in relation to the interface (i.e. W for west of the interface); the last number is the set number of the well (i.e. 1 for the first set).

To simulate the dissipation of the pore pressure in the arenaceous sediments, first the pore pressure dissipation at the interface (i.e., F/b) is found by fitting equation (28) to the groundwater level records of the eastern well with known L_e, K and S_s. The variable, $L_{e,}$ denotes the horizontal distance in the western-eastern direction between the interface and the well. The values of K and S_s are obtained from aquifer tests at the wells. Once the pore pressure dissipation at the interface is known and the east-west horizontal distance between the interface and the well, L_w, is given, the η value in equation (16) is determined by fitting equation (30) to the observed groundwater level of the western-side well. The bulk modulus of the fluid phase, C, is set to be 2.25×10^9 Pascal and the distance from the interface to the pinch-out, L, is set to be 30,000 meters.

According to the daily average records, the largest groundwater level changes in the wells are located at the interface between the gravels and the sands. To test the model, two well sets were chosen which include 3E1, 3W1, 3E2 and 3W2, shown in Figure 4(c). The records of wells 3E1 3E2 are fitted by equation (28), and the records of wells 3W1 and 3W2 are fitted using equation (30). Table 1 lists the best fitted parameters values and associated input parameter values. The simulated and observed ground water levels as a function of time are plotted in Figure 5 and Figure 6. In general, the agreements are excellent; the small differences between the observed records and the simulated results may be attributed to the simplified one-dimensional model as well as the no-leakage assumption. Records of another two sets of wells on the southern part of the fan were also analyzed, shown in Figure 4(b) and 4(c) as 3E3, 3W3, 2E1 and 2W1. Wells 3W3 and 2W1 are located at the same horizontal position with different screen depths. Simulated results for wells 3E3, 3W3, 2E1 and 2W1 are plotted against observed data (Figure 7). The observed dissipation of the pore pressure at well 2E1 is faster than simulated. This discrepancy may be attributed to the multidimensional diffusion process and leakage between aquifers, which were neglected in the one-dimensional model. Well 2E1 is located near location X as shown in Figure 4(c), which is a groundwater discharge area of the Cho-Shui River alluvial fan. A sudden increase of flow in the channel of the Cho-Shui River, downstream from X, was observed after the Chi-Chi earthquake [Water Conservancy Agency, 1999b]. According to the Water

Conservancy Agency report [2000] and Lee et al. [2002], the increase in river discharge was caused by groundwater discharge from Aquifer 1, resulting from the vertical water movement from Aquifer 2 to Aquifer 1. Since no aquitard exists between Aquifer 2 and Aquifer 1, the vertical water movement is significant. As a result, the reduction in the observed head of Aquifer 2 is much more rapid than the simulated water level at Well 2E1. The vertical water movement also may have occurred from Aquifer 3, but its magnitude may have been reduced by the aquitard found between Aquifers 2 and 3. The absence of the aquitard at Well 2E1 and its presence at Well 3E may provide a plausible explanation for the observed faster decrease of the ground water level at Well 2E1 (Figure 7), compared with the the simulated result. There is no significant difference between the observed and simulated hydrographs at Well 3E1 (Figure 5). Other evidence of vertical water movement can be found at location Y in Figure 4(c). At this location, an aquitard exists between Aquifers 2 and 3. This aquitard's eastern boundary is delineated in Figure 4(c), which resembles the shape of the contour of the ground water level changes in aquifer. The similarity in shape may suggest up-coning of the ground water in the area. Therefore, we conclude that the vertical water movement is significant in the unconfined aquifer of the fan.

A plot of η/C values obtained from the calibration and known L_w/K values is shown in Figure 8. These K values are those estimated from aquifer tests at the wells on the western side of the interface. A best fitted line is also shown, which is given as

$$\left(\frac{\eta}{C}\right) = 7.4x10^{-3}\left(\frac{L_{bc}}{K}\right) - 0.6\ . \tag{31}$$

The correlation coefficient is 0.96. The viscosity dissipation is proportional to the distance and inversely proportional to the hydraulic conductivity. Based on this relation, we surmise that the further the well is located from the interface, the less the well is affected by the viscosity dissipation. If hydraulic conductivity increases, viscosity coefficient η decreases and the dissipation of the pore pressure will occur quickly.

After the Chi-Chi earthquakes, liquefaction of the sediments was observed at several locations in the alluvial fan (see Fig. 5 (a)). The liquefaction was caused by high pore pressures induced by the earthquakes at the interface, and it's the subsequent pressure propagation throughout the aquifers. The phenomenon is analogous to a choke in open channel flow or a water hammer in pipe flow. Several liquefactions of sediments were observed at the upper fan (i.e., A, B1, B2 and B3 in Fig. 5a) where the aquifer is unconfined and strong vertical flow took place. Liquefaction of the sediment was also observed at the northern fan nearby the Taiwan Strait (see C and D in Fig. 5(a)). At the northern fan, no impermeable clay sediments have been found on top of the aquifer along the coastline. The absence of clay sediments is possibly due to wave erosion [Central Geological Survey, 1994, and 1999]. The excess pore pressure caused by the earthquake thus was released at these outlets and induced the liquefaction. But no sediment liquefaction was detected on the southern part of the fan which is also nearby the coastline, but much closer to the pinch-out.

This phenomenon appears to support our assumption of a zero strain rate at the pinch-out. Overall, the interface-induced high pore pressure increases the risk of sediment liquefaction, but the hydrogeology also plays an important role on the liquefaction potential. Finally, our analysis has demonstrated that the propagation of groundwater waves induced by the earthquakes is controlled by the geological structures and hydraulic properties of aquifers. The results of the analysis indicate that it is possible to use earthquake-induced groundwater changes to identify structures of groundwater basins and aquifer heterogeneity. Groundwater level changes caused by earthquakes from different epicenters may provide data sets of naturally-occurring hydraulic tomography surveys of the aquifers -- surveys that are analogous to the hydraulic tomography proposed by Yeh and Liu [2000] and Liu et al. [2002].

5. Conclusion

This study developed a visco-elastic model to describe the pore pressure dissipation after impulse pressures induced by two significant earthquakes. This model was used to reproduce the post-earthquake groundwater level changes observed in the monitoring wells in the Cho-Shui River alluvial fan. Once the direction of the wave propagation was known, using the observed groundwater level changes in two monitoring wells in the direction of the wave propagation, and the interface position of sand and gravel formation in the confined aquifer, the viscosity coefficient of the model was estimated. Using this approach, the only

data required is the hydraulic conductivity and the specific storage, both of which are obtained by the field tests; knowledge of the magnitude of the earthquake is unnecessary. Results of the study show that the estimated viscosity coefficient is strongly correlated to the hydraulic conductivity of the aquifer. Most importantly, our study shows that geological heterogeneity plays a significant role in ground water level changes and sediment liquefactions induced by earthquakes. Our study may catalyze the use of earthquake-induced ground water level changes to delineate large-scale aquifer heterogeneity and geological structures.

Acknowledgements

This study was supported by the National Science Council of TAIWAN under contract No. NSC 89-2116-M-002-053. The authors are grateful to the Water Resources Agency and the Central Geological Survey of TAIWAN for providing the field data. The third author is funded by NSF and SERDP of USA by a grant EAR-0229717. The authors also extend their gratitude to Martha P.L. Whitaker for her editing of this document.

References

Bardet, J. P., A viscoelastic model for the dynamics behavior of saturated pore-elastic solids, Journal of Applied Mechanics, 59, 128-135, 1992.

Berryman, J. G., L. Thigpen, and C. T. Chin, Bulk elastic wave propagation in partially saturated porous solids, The Journal of the Acoustical Society of America; 4, 360-373, 1988.

Biot, M. A., Theory of propagation of elastic waves in a fluid-saturated porous solid, I. low-frequency range, The Journal of the Acoustical Society of America, 28, 168-178, 1956a.

Biot, M. A., Theory of propagation of elastic waves in a fluid-saturated porous solid, II. high-frequency range, The Journal of the Acoustical Society of America, 28, 179-191, 1956b.

Biot, M. A., General theory of three-dimensional consolidation, Journal of Applied Mechanics, 12, 155-164, 1941.

Central Geological Survey, The hydrogeological survey report of the Cho-Shui alluvial fan, Ministry of Economic Affairs, Taiwan, 1999. (in Chinese)

Central Geological Survey, The final survey report of the Cho-Shui alluvial fan, Ministry of Economic Affairs, Taiwan, 1994. (in Chinese)

Chia, Y. P., Y. S. Wang, J. J. Chiu, and C. W. Liu, changes of groundwater level due to the 1999 Chi-Chi earthquake in the Choshui River alluvial fan in Taiwan, Bulletin of the

Seismological Society of America, 91, 1062-1068, 2001.

Chia, Y. P., Y. S. Wang, H. P. Wu, C. J. Huang, C. W. Liu, M. L. Lin, and F. S. Jeng, Changes of ground water level in response to the Chi-Chi earthquake, in, Proceedings of International Workshop on Annual Commemoration of Chi-Chi Earthquake, vol. I – Science Aspect, edited by Loh, C. H., and W. I. Liao, pp. 317-328, National Center for Research on Earthquake Engineering, Taiwan, 2000.

Coleman, B. D., and W. Noll, The thermodynamics of elastic materials with heat conduction and viscosity, Archive for Rational Mechanics and Analysis, 13, 167-178, 1963.

Drew, D. A., and S. L. Passman, Theory of multicomponent fluids, 308 pp., Springer Verlag New York Inc., New York, 1999.

Department of Land Administration, The records of the first and the second class GPS control stations, Ministry of the Interior, 2000. (digital records)

Eringen A. C., Mechanics of continua, 592 pp., R. E. Krieger Pub. Co., Huntington, New York 1980.

Farrell, O. J., and B. Ross, Solved problems: Gamma and Beta functions, Lendre polynomials, Bessel functions, 410 pp., Dover Publications, New York, 1971.

Flügge, W., Viscoelasticity, 194 pp., Springer-Verlag, New York, 1975.

Ge, S., and S. C. Stover, Hydrodynamic response to strike- and dip-slip faulting in half space, Journal of Geophysical Research, 105(B11), 25513-25524, 2000.

Grecksch, G., F. Roth, and H. J. Kumpel, Cosesmic well level changes due to 1992 Roermond earthquake comparing to static deformation of half space solutions, Geophysical Journal International, 138, 470-478, 1999.

Green, and P. M. Naghdi, A dynamical theorem of interacting continua, International Journal of Engineering Science, 3, 241, 1965.

Hassanizadeh, M., and W. G. Gray, General conservation equations for multi-phase systems: 3. constitutive theory for porous media flow, Advances in Water Resources, 3, 25-40, 1980.

Hassanizadeh, M., and W. G. Gray, General conservation equations for multi-phase systems: 1. averaging procedure, Advances in Water Resources, 2, 131-144, 1979a.

Hassanizadeh, M., and W. G. Gray, General conservation equations for multi-phase systems: 2. mass, momenta, energy, and entropy equations, Advances in Water Resources, 2, 191-203, 1979b.

Hsu, S. K., Plan for a groundwater monitoring network in Taiwan, Hydrogeology Research, 6, 405-415, 1998.

Huang, B. S., Two dimensional reconstruction of the surface ground motion of an earthquake: the September 21, 1999, Chi-Chi, Taiwan earthquake, Geophysical Research Letters, 27, 3025-3028, 2000.

Jeng, D. S., and T. L. Lee, Dynamic response of porous seabed to ocean waves, Computers and Geotechnics, 28, 99-128, 2001.

Lamb, S H. Hydrodynamics, 738 pp., Dover Publications, New York, 1945.

Lee, M., T. K. Liu, K. F. Ma, and Y. M. Chang, Coseismic hydrological changes associated with dislocation of the September 21, 1999 Chichi earthquake, Taiwan, Geophysical Research Letters, 29, art. no. 1824, 2002.

Lin, Y. P., Y. C. Tan, and S. Rouhani, Identifying spatial characteristics of transmissivity using simulated annealing and kriging methods, Environmental Geology, 41, 200-208, 2001.

Lin, Y. P., C. C. Lee, and Y. C. Tan, Geostatistical approach for identification of transmissivity structure at Dulliu area in Taiwan, Environmental Geology, 40, 111-120, 2000.

Liu, S. Y., T. -C. J. Yeh and R. Gardiner, Effectiveness of Hydraulic Tomography: Numerical and Sandbox Experiments, Water Resources Research, 38, 10.1029/2001WR000338, 2002.

Ma, K. F., J. Mori, S. J. Lee, and S. B. Yu, Spatial and temporal distribution of slip for the 1999 Chi-Chi, Taiwan, earthquake, Bulletin of the Seismological Society of America, 91, 1069-1087, 2001.

Ma, K. F., C. T. Lee, and Y. B. Tsai, The Chi-Chi, Taiwan earthquake: large surface displacement on an inland thrust fault, Eos (Transactions, American Geophysical Union), 80, 605-611, 1999.

Ohno, M, and H. Wakita, A water well sensitive to seismic waves, Geophysical Research Letters, 24, 691-694, 1997.

Prevost, J. H., Nonlinear transient phenomena in saturated porous media, Computer Methods

in Applied Mechanics and Engineering, 20, 3-18, 1982.

Roeloffs, E. A., Persistent water level changes in a well near Park field, California, due to local and distant earthquakes, Journal of Geophysical Research, 103, 869-889, 1998.

Roeloffs, E. A., Poroelastic techniques in the study of earthquake-related hydrologic phenomena, in, Advances in Geophysics, 37, 135-195, edited by Dmowska, R., and B. Saltzman, Academic Press, New York, 1996.

Wang, C. C., A new presentation theorem for isotropic functions, part I. Archive for Rational Mechanics and Analysis, 36, 166-197, 1970a.

Wang, C. C., A new presentation theorem for isotropic functions, part II. Archive for Rational Mechanics and Analysis, 36, 198-233, 1970b.

Wang, C. Y., L. H. Cheng, C. V. Chin, and S. B. Yu, Coseismic hydrologic response of an alluvial fan to the 1999 Chi-Chi earthquake, Taiwan, Geology, 29, 831-834, 2001.

Water Conservancy Agency, Analysis for the changes of surface levels and ground water levels caused by the 921 Chi-Chi earthquake, Ministry of Economic Affairs, Taiwan, 2000. (in Chinese)

Water Conservancy Agency, The annual report of the Groundwater Monitoring Network System (GMNS) records in Taiwan, Ministry of Economic Affairs, Taiwan, 1999a. (in Chinese)

Water Conservancy Agency, The annual report of the daily flow records in Taiwan, Ministry

of Economic Affairs, Taiwan, 1999b. (in Chinese)

Yeh, T.-C. J. and S. Y. Liu, Hydraulic tomography: development of a new aquifer test method, Water Resources Research, 36, 2095-2105, 2000.

Yu, S. B., L. C. Kuo, Y. J. Hsu, H. H. Su, C. C. Liu, C. S. Hou, J. F. Lee, T. C. Lai, C. C. Liu, C. L. Liu, T. F. Tseng, C. S. Tsai, and T. C. Shin, Preseismic deformation and coseismic displacement associated with the Chi-Chi, Taiwan, earthquake, Bulletin of the Seismological Society of America, 91, 995-1012, 2001.

Captions

Table

1. The fitting parameters and hydraulic properties of the wells used in this study

Figures

1. The geology and geography of the study area
2. Hydrogeology of the study area and the conceptual model
3. The distribution of ground water level changes right after the Chi-Chi earthquake
4. Changes in ground water level, hydraulic conductivity distribution, and the locations of the interface, pinch-out, and observed liquefaction area
5. The comparison of observed and simulated groundwater level in the wells 3E1 and, 3W1
6. The comparison of observed and simulated groundwater level in the wells 3E2 and, 3W2
7. The comparison of observed and simulated groundwater level in the wells 3E3, 3W3, 2E1 and 2W1
8. The regression relationship of $\frac{\eta}{C}$ and $\frac{L_w}{K}$, and the 95% confidence interval of the regression

Table 1. The fitting parameters and hydraulic properties of the wells used in this study
*Data obtained by the well pumping tests. [Water Conservancy Agency, 1999a]

Well No.	L_e or L_w (m)	Position (TM2D, central meridian = 121°E)		Specific storage S_s (1/m)*	Hydraulic conductivity K (m/day)*	The horizontal distance between the eastern well and the western well (m)	$\frac{\eta}{C}$ (day)
2E1	0	185350	2624184	0.80e-4	12.355	6682	0.19
2W1	6600	178717	2624989		30.499		
3E1	450	194052	2656100	1.50e-4	26.870	3934	0.64
3W1	3500	190120	2656250		56.572		
3E2	2000	196133	2649778	2.30e-4	52.445	8613	0.00025
3W2	6000	187624	2648441		67.133		
3E3	680	191168	2627781	0.50e-4	29.894	12746	7.2
3W3	12000	178717	2624989		11.568		

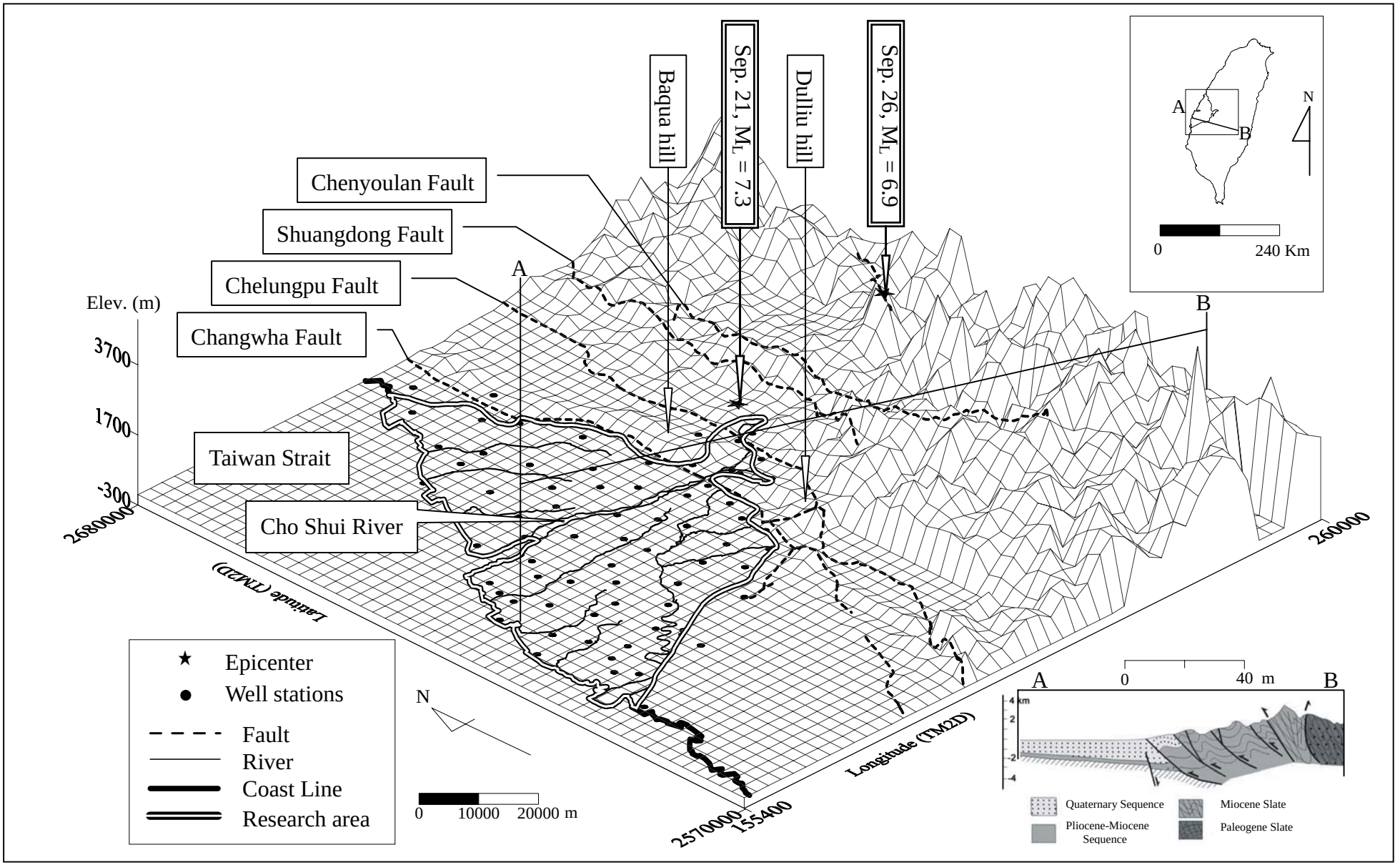

Figure 1. The geology and geography of the study area

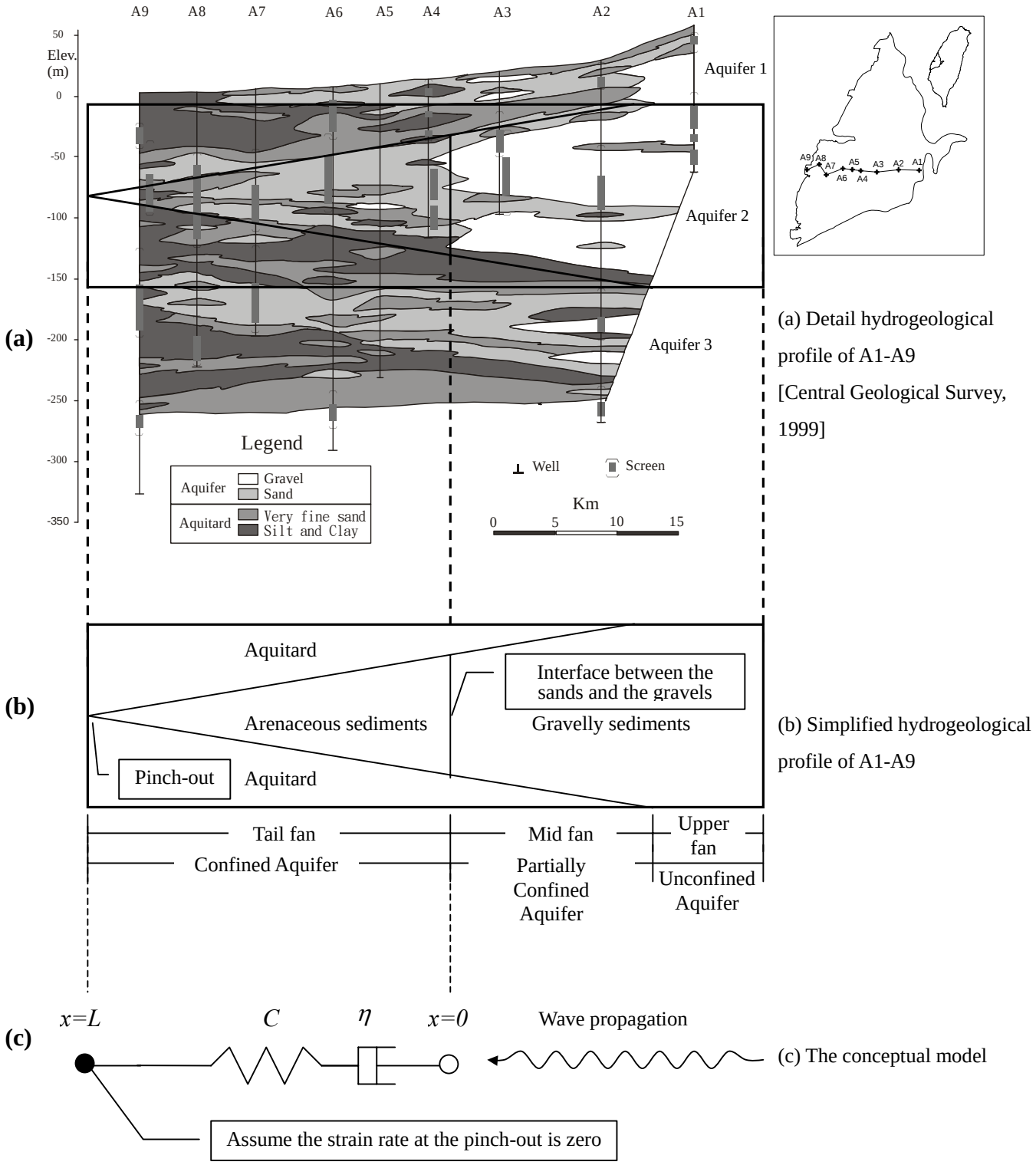

Figure 2. Hydrogeology of the study area and the conceptual model

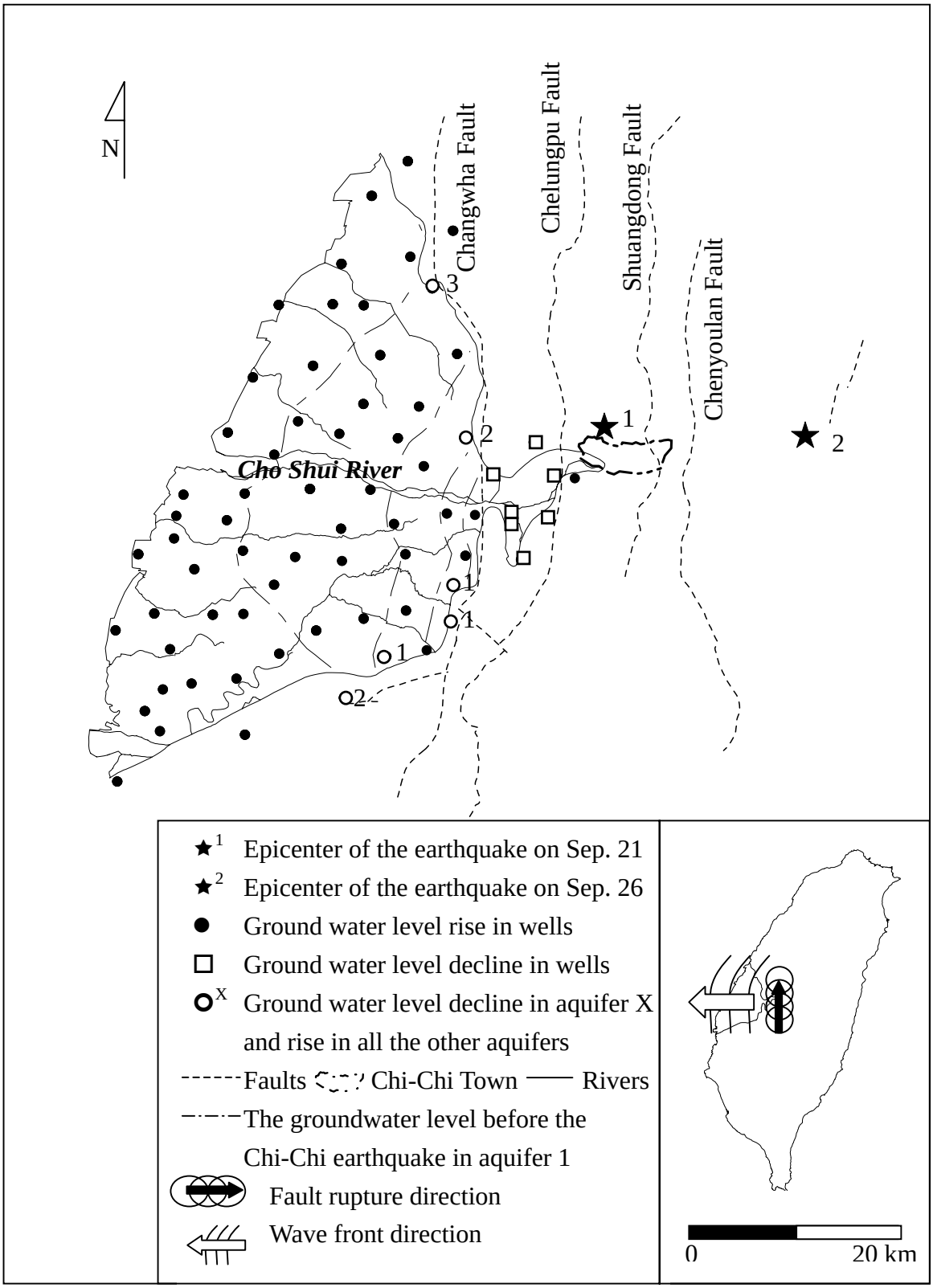

Figure 3. The distribution of ground water level changes right after the Chi-Chi earthquake

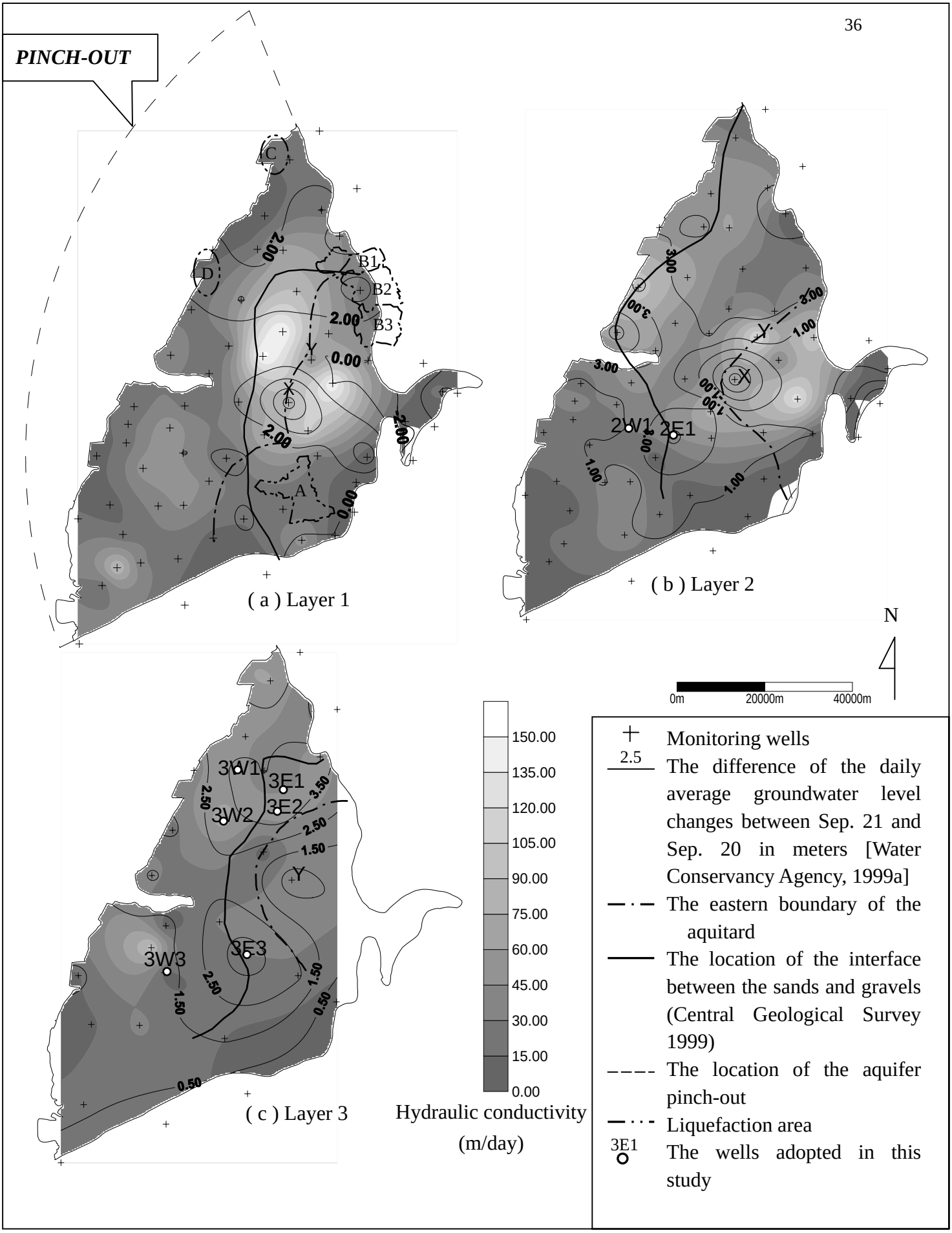

Figure 4. Changes in ground water level, hydraulic conductivity distribution, and the locations of the interface, pinch-out, and observed liquefaction area

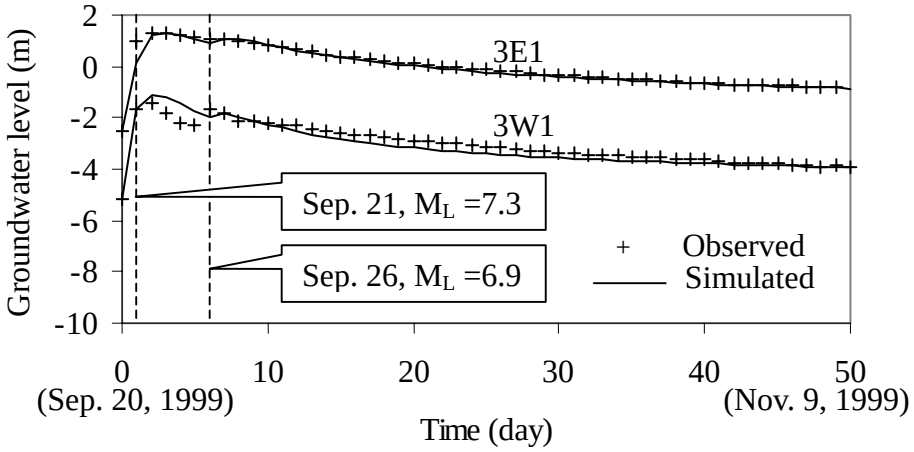

Figure 5. The comparison of observed and simulated groundwater level in the wells 3E1 and, 3W1

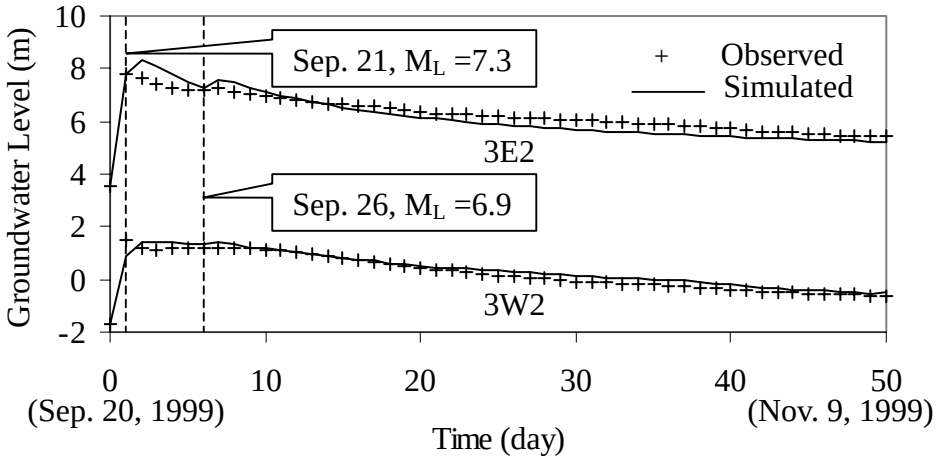

Figure 6. The comparison of observed and simulated groundwater level in the wells 3E2 and, 3W2

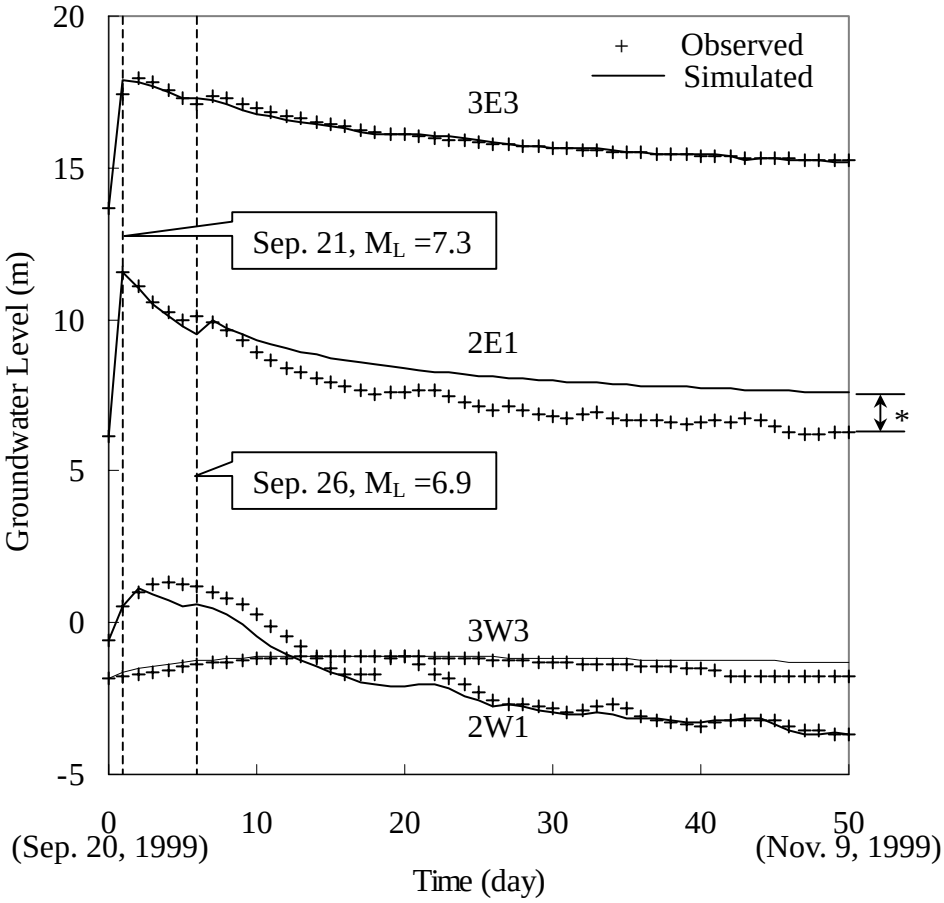

* This discrepancy may be attributed to a multidimensional diffusion process and leakage between aquifer, which were neglected in the one-dimensional model.

Figure 7. The comparison of observed and simulated groundwater level in the wells 3E3, 3W3, 2E1 and 2W1

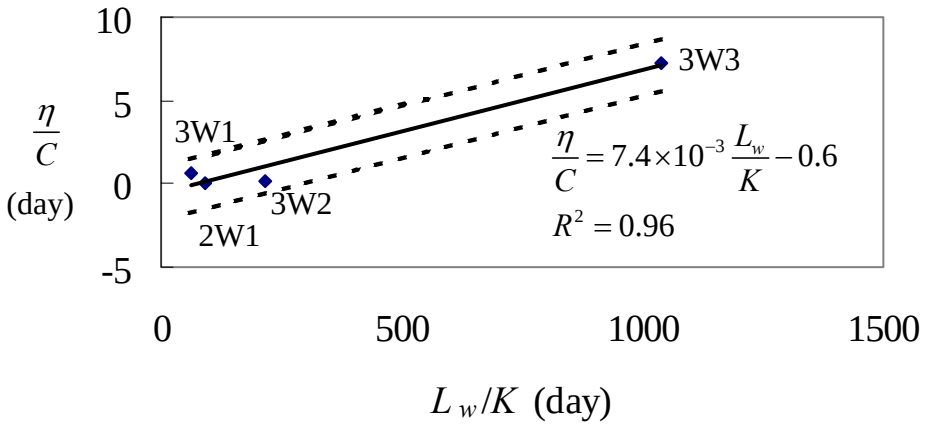

Figure 8. The regression relationship of $\frac{\eta}{C}$ and $\frac{L_w}{K}$, and the 95% confidence interval of the regression